World Applied Sciences Journal 35 (3): 483-499, 2017
ISSN 1818-4952

DOI: 10.5829/idosi.wasj.2017.483.499

Investigating the Behavior of an Existing Quay Wall Using the Characteristic Parameters of Port-Said Clay, Egypt

[1]Omaima M. Hamed, [1]Mohamed F. Mansour, [2]Ahmed H. Abdel-Rahman and [1]Fathalla M. El-Nahhas

[1]Ain Shams University, Egypt
[2]National Research Center, Egypt

Abstract: Construction in soft clays poses multiple challenges to engineering design. Soft clays are characterized by low strength, high compressibility and time-dependency of deformations. In Northeastern Egypt, the East of Port-Said region is characterized by extended deposits of very soft to firm clays known as Port-Said Clay. This paper presents a numerical study on the three-dimensional interaction between Port-Said Clay and an existing quay wall at East Port-Said Port. Both the Hardening Soil Model (HSM) and the Soft Soil Creep Model (SSCM) were utilized. The results highlighted the paramount significance of considering not only the undrained and drained properties, but also the secondary consolidation effects on the deformation behavior of the Quay wall. The long-term horizontal and vertical movement increments due to secondary consolidation reached 25% and 139%, respectively. The results also showed that the horizontal wall movements are overestimated in two-dimensional analyses by up to 22% when considering secondary consolidation.

Key words: Soft marine clays · Port-Said Clay · Hardening Soil Model · Soft Soil Creep Model · Quay Walls · Secondary consolidation

INTRODUCTION

Soft clays are considered among the most problematic soils due to their low strength, high compressibility and time dependency of deformations. Hence, their interaction with different structures incurs many complexities in terms of engineering behavior both in the short and long-term conditions.

Soft clays are generally deposited in low-elevation delta plains formed at the mouth of rivers where the water slows down, thereby allowing for the slow deposition of the fine clay particles. In Egypt, the Nile River flows from the south and forms its delta in Northern Egypt extending from the east of Alexandria city to Port-Said city. Old branches of the Nile River formed a wider delta plain in Northeastern Egypt extending to the east of the city of Port-Said, which is known as El-Tina Plain. Figure 1 shows the location of El-Tina Plain on Egypt's map.

The Egyptian government has ambitious plans for major development in the East of Port-Said region by creating logistic zones to serve the international trade passing through Suez Canal. Soft clays in this region extend to more than fifty meters below the natural ground surface. Many geological studies had focused on the history of deposition of Northern Nile Delta in general and El-Tina Plain in particular (Weir *et al*. [2]; Ibrahim [3]; Stanley [4]; Abdeltawab and Hussein [5]; Barakat [6]; and Ismail and Ryden [7]). These studies suggested that the soft clays in this region were all deposited in similar geological conditions. Hence, it is believed that their engineering properties are also similar.

The soft marine clays of El-Tina Plain did not, however, receive the same level of attention from the geotechnical researchers, probably due to the absence of previous development plans in the area. Previous geotechnical engineering studies were all carried out as part of specific engineering projects.

Comprehensive in-situ and laboratory testing programs have been carried out in the present research in order to characterize the soft marine clays in El-Tina Plain, called hereinafter "Port-Said Clay". The outcome of this characterization was presented in details by Hamed *et al*. [8]. In this paper, the undrained (short-term) and drained (long-term) deformation behaviors of an existing quay wall at the East Port-Said Port were investigated in a three-dimensional (3D) model using the parameters developed

Corresponding Author: Mohamed F. Mansour, El Sarayat Street, Abassia, Cairo, Egypt 11517.
Cell: +20 109 981 5877

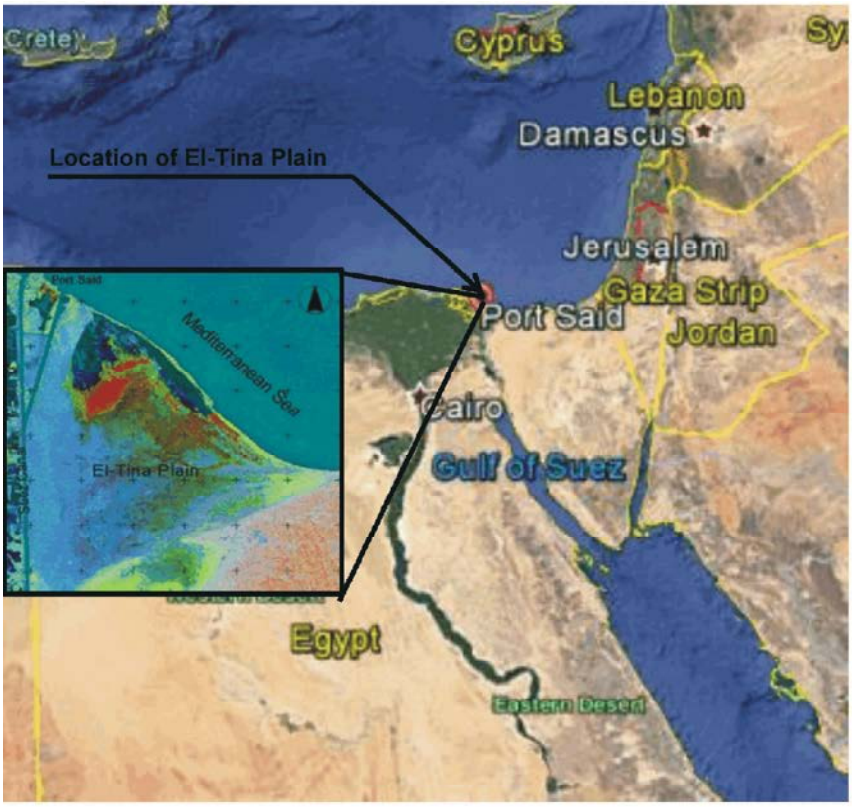

Fig. 1: Location of El-Tina plain on Egypt's map (Sources: Google Earth© and El Gammal [1])

for Port-Said Clay [8]. The constitutive behavior of Port-Said Clay was represented by the Hardening Soil Model (HSM) and the Soft Soil Creep Model (SSCM) in order to quantify the contribution of secondary consolidation to the total deformation. The parameters of the two constitutive models were determined from the results of the in-situ and laboratory tests carried out on Port-Said Clay. Additional two-dimensional analyses have also been conducted to provide design recommendations.

Geology of the Area: Port-Said Clay is deposited in El-Tina plain, which is composed of soft marine clays extending to more than fifty meters below the ground surface. The origin of Port-Said Clay is related to one of the old Nile River tributaries during the Holocene time, which is named the Pelusiac branch. During the Pleistocene and Holocene, the Nile Delta had more tributaries than it currently has, but these tributaries disappeared gradually due to flood control measures and the subsequent silting up. The Pleistocene and Holocene formations cover about 16% of Egypt's area including Port-Said region. During the Pleistocene, the sea level fluctuated and sometimes flooded parts of the Nile Delta but retreated other times from it. The Red Sea Mountains were the main source of water reaching the Nile. The tributaries originating from the Red Sea Mountains carried large amounts of silt towards the Nile. The Holocene deposits included both marine deposits and fluvio-marine deposits composed of clay and sandy clay with biotite and magnetite (Abu-Al-Izz [9]). Therefore, they have a dark gray color. The Quaternary deposits at El-Tina plain, where Port-Said Clay is found, consist of a number of sedimentation cycles of sand, clay and silt. El-Tina bay was formed due to the interface of seawater and the Nile water at the Northwest corner of Sinai about 1000 BC. The transgression and regression of the sea formed the huge salty clay and silt deposit (Abdallah [10]).

Subsurface Conditions: Hamed *et al*. [8] developed an idealized profile representing the subsurface conditions at El-Tina plain, as shown in Figure 2. The idealized profile consisted of fill in the depth range of 0.0 to 1.75 m, silty sand in the depth range of 1.75 to 2.6 m, an upper clay in the depth range of 2.6 to 3.4 m, silty sand in the depth range of 3.4 to 7.6 m, a lower clay in the range of 7.6 to 51.6 m and sand in the range of 51.6 to 55.0 m or deeper.

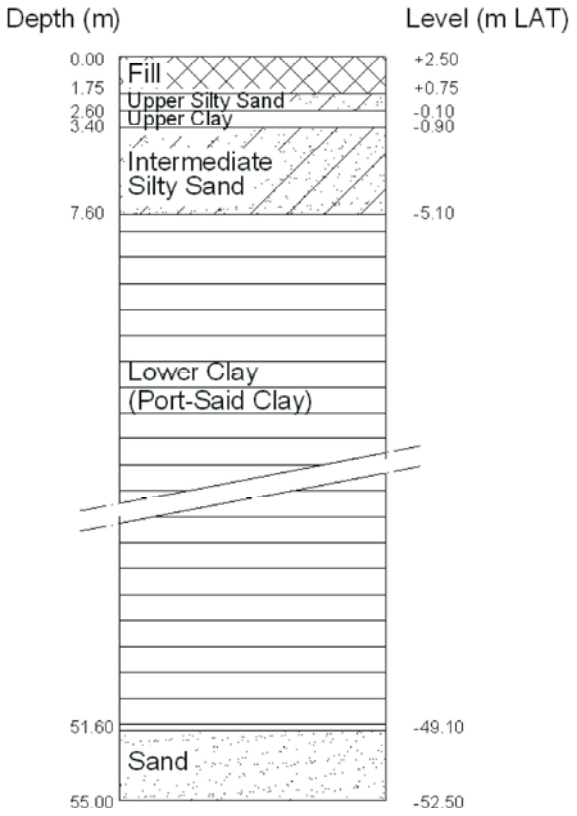

Fig. 2: Idealized profile for El-Tina Plain at the location of maximum depth of Port-Said Clay

It is considered that the main Port-Said Clay deposit is represented by the lower clay. The groundwater table was encountered at depths ranging from 1.3 to 4.3 meters. The corresponding levels are referenced in Figure 2 to the Lowest Astronomical Tide (LAT) datum.

Constitutive Models Parameters: Two constitutive soil models were chosen to describe Port-Said Clay behavior: the Hardening Soil Model (HSM) and the Soft Soil Creep Model (SSCM). These two models are selected in order to highlight the important role of the elasto-plastic yielding as well as the secondary consolidation on the deformation behavior of soft soils in the long-term conditions.

Hardening Soil Model (HSM): The hardening soil model (HSM), developed by Schanz *et al*. [11], was formulated within the framework of the theory of plasticity. The HSM accounts for the effects of unloading and reloading on the soil stiffness, the soil dilatancy and introduces a yield cap. The model accounts for both shear and volumetric compression hardening. Shear hardening takes place due to primary deviatoric loading, while volumetric compression hardening takes place due to isotropic loading and primary compression in the oedometer loading condition. The yield conditions can be defined using the Mohr-Coulomb failure criterion.

The soil stiffness in the primary loading condition is presented by a power law, as shown in Equation (1).

$$E_{50} = E_{50}^{ref}\left(\frac{\sigma'_3 + c\cot\phi}{p^{ref} + c\cot\phi}\right)^m \quad (1)$$

Where E_{50} is the elastic deformation modulus for a mobilization of 50% of the maximum deviator stress (q_f); E^{ref}_{50} is the reference stiffness modulus corresponding to a reference confining stress, p^{ref}, of 100 kPa; c & ϕ are the drained shear strength parameters of Mohr-Coulomb failure criterion; σ_3' is the effective confining pressure; and m is a power exponent

The effect of unloading and reloading on the soil stiffness is also described by a power law, as shown in Equation (2).

$$E_{ur} = E_{ur}^{ref}\left(\frac{\sigma'_3 + c\cot\phi}{p^{ref} + c\cot\phi}\right)^m \quad (2)$$

Where E_{ur} is the unloading-reloading deformation modulus; and E^{ref}_{ur} is the reference unloading-reloading deformation modulus corresponding to a reference confining stress, p^{ref}, of 100 kPa.

Another basic characteristic of the HSM is the consideration of the plastic straining due to primary compression, which can be defined as follows:

$$E_{oed} = E_{oed}^{ref}\left(\frac{\sigma'_1 + c\cot\phi}{p^{ref} + c\cot\phi}\right)^m \quad (3)$$

Where E_{oed} is the tangent deformation modulus for primary loading; E^{ref}_{oed} is the reference tangent deformation modulus corresponding to a reference vertical stress p^{ref} of 100 kPa; and σ_1' is the effective vertical pressure.

The deformations are controlled in the HSM by three stiffness parameters that simulate loading (E_{50}), unloading-reloading (E_{ur}) and the oedometer loading conditions (E_{oed}). The results of sixteen (16) consolidated-undrained triaxial (with pore water pressure measurements) and oedometer tests presented by Hamed *et al*. [8] were utilized to define the different stiffness parameters of the HSM for Port-Said Clay. The relation between the undrained deformation modulus at 50% of the failure deviatoric stress (E_{u50}) and the normalized effective confining pressure, i.e. σ_3'/p_a, is

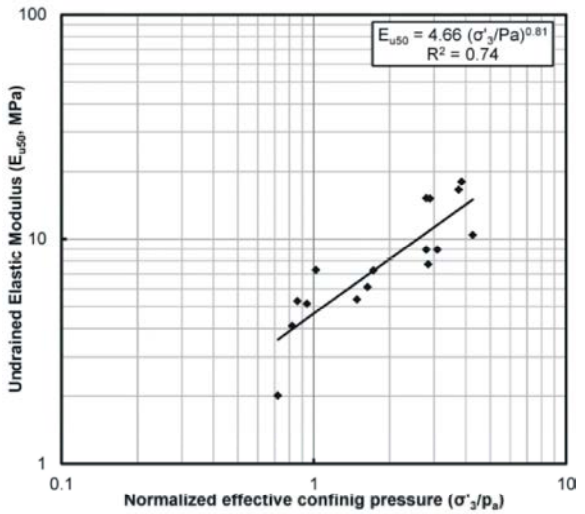

Fig. 3: Variation of E_{u50} with the effective confining stress (σ_3') illustrating the power law trend equation

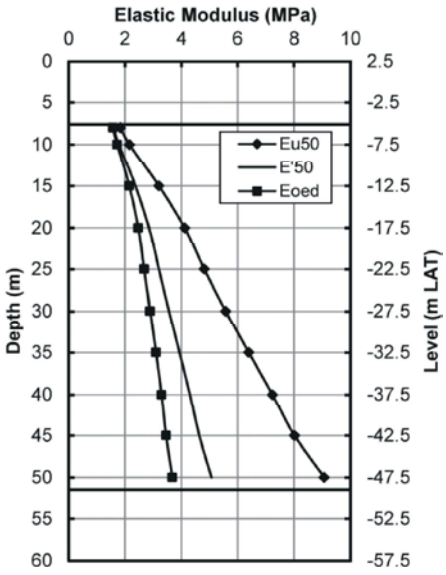

Fig. 4: Variations of E_{u50}, E'_{50} and E_{oed} with depth for Port-Said Clay

presented in Figure 3. Therefore, E_{u50} can be expressed in terms of the effective confining pressure (σ_3') through Equation (4) for Port-Said Clay.

$$E_{u50} = 4.66\left(\frac{\sigma'_3}{100}\right)^{0.81} \quad (4)$$

Similarly, the results of the conducted consolidated-drained triaxial tests indicated that the drained modulus at 50% of the failure stress (E'_{50}) can be expressed as shown in Equation (5).

$$E'_{50} = 3.12\left(\frac{\sigma'_3}{100}\right)^{0.59} \quad (5)$$

Hamed *et al*. [8] concluded that the unloading-reloading modulus (E_{ur}) can be taken 7 times the value of the undrained modulus (E_{u50}). The results of the consolidation tests were also utilized to calculate the reference-constraint modulus (E^{ref}_{oed}) of Port-Said Clay at a reference effective vertical stress of 100 kPa. The reference-constrained modulus was found to be equal to 2.1 MPa.

The value of the at-rest earth pressure coefficient (K_o) was calculated from the correlation developed by Massarsch [12] for normally consolidated clays; i.e. $K_o = 0.44 + 0.0042$ PI. Hamed *et al*. [8] found that the plasticity index (PI) of Port-Said Clay increases with depth according to a linear correlation, as shown in Equation (6).

$$PI(\%) = 30 + [z(m) - 7.6] \text{ for } z \geq 7.6 \text{ m} \quad (6)$$

Hence, the variation of K_o with depth was also considered. Figure 4 shows the variations with depth of each of the undrained modulus (E_{u50}), the drained modulus (E'_{50}) and the constraint modulus (E_{oed}) for Port-Said Clay. The upper and lower elevation boundaries of Port-Said Clay are also shown in the form of horizontal solid bold lines.

Hamed *et al*. [8] determined the effective shear strength parameters c' = 0 kPa and ϕ' = 22°. The failure ratio (R_f) was calculated from Duncan-Chang equations (Duncan and Chang [13]) and it was found equal to 0.85.

Soft Soil Creep Model (SSCM): Roscoe *et al*. [14] formulated a stress-strain model for normally-consolidated or lightly over-consolidated clays. The model is known as the Cam Clay Model and it was formulated within the framework of the strain hardening theory of plasticity. Later, Burland [15] suggested a modified version of the Cam Clay model based on the Critical State Theory, which is known as the Modified Cam Clay Model. The non-linear behavior of soil is modeled by the means of hardening plasticity. The stress-dependency of stiffness (logarithmic compression behavior) is also considered.

The Soft Soil Creep Model (SSCM) accounts for the volumetric creep characteristics, i.e. secondary consolidation, which is very important in soft normally consolidated clays. The SSCM also makes a clear distinction between primary loading and the unloading-reloading conditions. The failure conditions are controlled by Mohr-Coulomb failure criterion. The basic parameters

of the SSCM are the failure parameters (c' and ϕ'), the modified swelling index, κ*, the modified compression index, λ* and the modified creep index, μ*. The last three parameters are related to the compression and swelling indices (C_c and C_s, respectively) and the coefficient of secondary consolidation (C_α) according to Equations (7) to (9), as follows:

$$\lambda^* = \left(\frac{C_c}{2.3(1+e_o)} \right) \quad (7)$$

$$\kappa^* = \left(\frac{2C_s}{2.3(1+e_o)} \right) \quad (8)$$

$$\mu^* = \left(\frac{C_\alpha}{2.3(1+e_0)} \right) \quad (9)$$

Results of the one-dimensional consolidation tests presented by Hamed *et al*. [8] were utilized to determine the different SSCM parameters for Port-Said Clay. The compression index (C_c) ranged from 0.6 to 0.9 and a characteristic value of 0.75 was considered. The swelling index (C_s) was found to be 0.14 C_c. Therefore, a design value of 0.105 for the swelling index was considered.

A simplified statistical analysis revealed that a characteristic value of 0.014 can be adopted for the coefficient of secondary consolidation (C_α) of Port-Said Clay. The initial void ratio (e_o) of Port-Said Clay was taken 2.0 according to the physical properties tests results reported by Hamed *et al*. [8]. Hence, the utilized values for the modified compression index (λ*), the modified swelling index (κ*) and the modified creep index (μ*) were 0.109, 0.03 and 0.002, respectively.

Case Study: The case study under investigation is the existing quay wall at the East Port-Said Port. The first phase of the port involved the construction of a 1200m-long quay wall located about 1300 m east of the Suez Canal bypass and at a distance of 1000 m from the Mediterranean Sea shoreline (Hamza *et al*. [16]).

The structural system of the quay wall – shown in Figure 5 – consisted of two main walls; the front wall and the back wall. The two walls are 35m-apart, which represents the width of the deck structure. They are connected by a series of transverse barrettes, a group of main beams and a cast in-situ slab at the top. The front 1.0 m-thick diaphragm wall provides support along the dredge side down to the depth of 34.5 m (-32 m LAT). The back diaphragm wall had the same thickness and extended down to a depth of 10.5 m, i.e. -8 m LAT (Hamza *et al*. [16]).

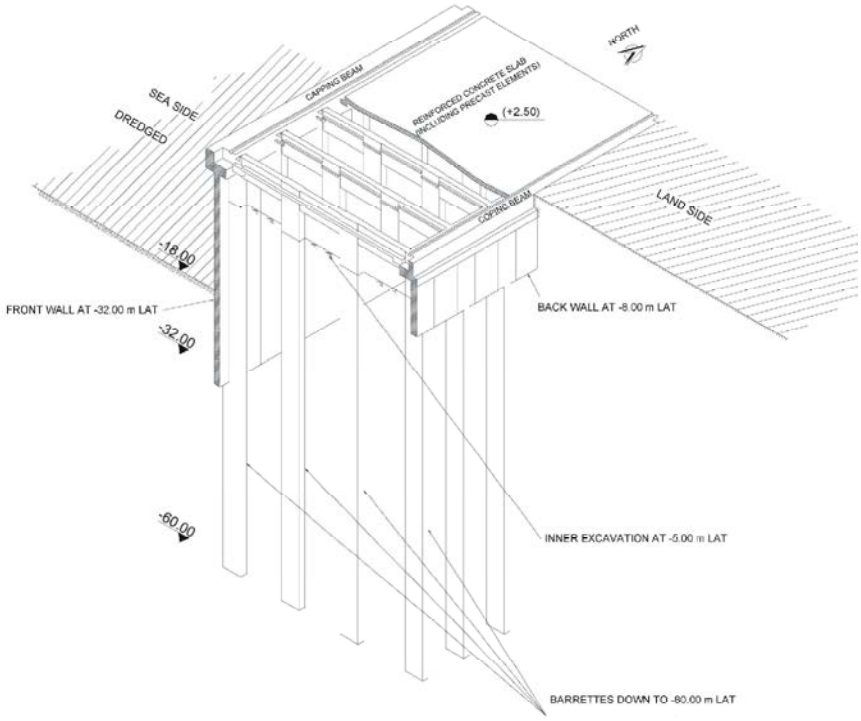

Fig. 5: Isometric view of the quay wall at East Port-Said Port (modified after Hamza *et al*. 2002)

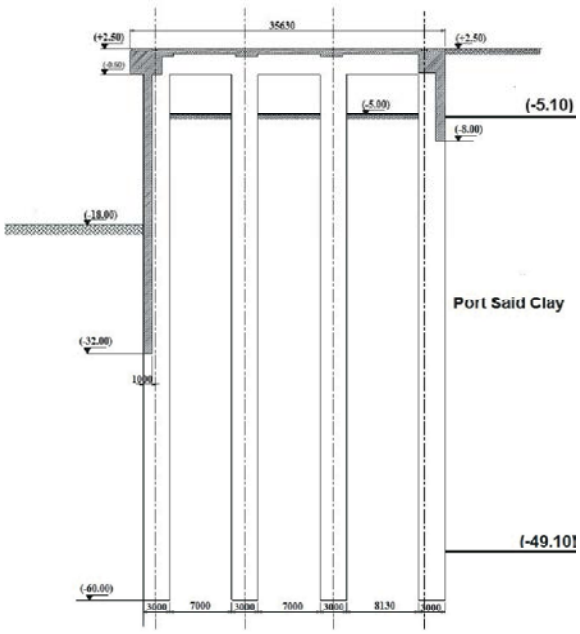

Fig. 6: Sectional elevation in the quay wall of East Port-Said Port (modified after Hamza *et al*. 2002)

The transverse barrettes extended down to the depth of 62.5 m (-60 m LAT). Each barrette had dimensions of 3 x 1 m and the spacing between the barrettes in the series ranged from 10 to 11 m. The series of four barrettes was repeated every 7 m in the parallel direction to the 1200 m-long quay wall. The main beam was 0.8 m-wide and 3 m-deep. A longitudinal seaside front beam having dimensions of 3.5 x 3.0 m and another back beam with dimensions of 3 x 3 m at the end of the deck were designed and constructed to support the system. Figure 5 shows an isometric view of the quay wall system illustrating the elevations of the different elements of the quay wall system referenced to the Lowest Astronomical Tide (LAT). A sectional elevation of the system is illustrated in Figure 6.

Numerical Analysis of East Port-said Port's Quay Wall: The deduced parameters of Port-Said Clay according to the HSM and the SSCM were employed to numerically simulate its interaction with the quay wall system. The analysis was carried out in the undrained (short-term) and drained (long-term) conditions. The finite element-based PLAXIS-3D Foundation software was utilized to develop the numerical model and carry out the analyses.

Analysis Approach: The effective stress approach was adopted in carrying out the numerical simulations in the undrained and drained conditions. Hence, the effective shear strength parameters (c' and ϕ') were considered in all the analyses. The undrained (short-term) behavior of the quay wall was investigated by employing the HSM and the associated undrained deformation modulus. The fully drained (long-term) behavior was investigated utilizing the HSM and the SSCM in order to quantify the contribution of secondary consolidation to the overall deformations.

Numerical Model Description: The problem under study necessitated developing a model with plan dimensions of 121 x 14 m and a depth of 82.5 m, as shown in Figure 7 and Figure 8. The perpendicular plan dimension was chosen 14 meters to represent twice the spacing between the barrettes. The top boundary of the model was free in all directions, while the bottom boundary of the model was fixed in all directions. The side boundaries were located at 20 and 70 m from the centerline of the front and back walls, respectively. The side boundaries were restrained in the horizontal directions normal to the model face.

Multiple horizontal work planes were created at the following levels in order to define the construction phases:

- +2.5 m LAT for the top level of the deck;
- +0.0, -2.5 and -5.0 m LAT for the successive excavation levels under the deck and in front of it;
- -8.0, -11.0, -14.5 and -18.0 m LAT for the dredging stages at the sea side;
- -8.0 and -32.0 m LAT for the tip levels of the back and front diaphragm walls, respectively;
- -60.0 m LAT for the average tip level of the barrettes; and
- -80.0 m LAT for the bottom boundary of the numerical model.

The three-dimensional domain was created by generating two-dimensional (2D) meshes at different planes followed by developing the three-dimensional (3D) mesh (Figures 7 and 8). The investigated domain was divided into 15-node wedge elements, which were composed of 6-node triangular faces in the work horizontal planes and 8-node quadrilateral faces in the vertical direction.

Compatible 6-node plate elements and 16-node interface elements were utilized to model the structural behavior and the soil-structure interaction, respectively. The roughness of the structural elements was modeled by assigning a suitable value for the interface strength reduction factor (R_{inter}).

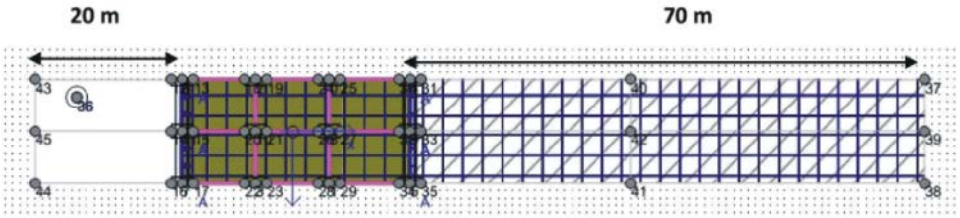

Fig. 7: Plan view of the developed model

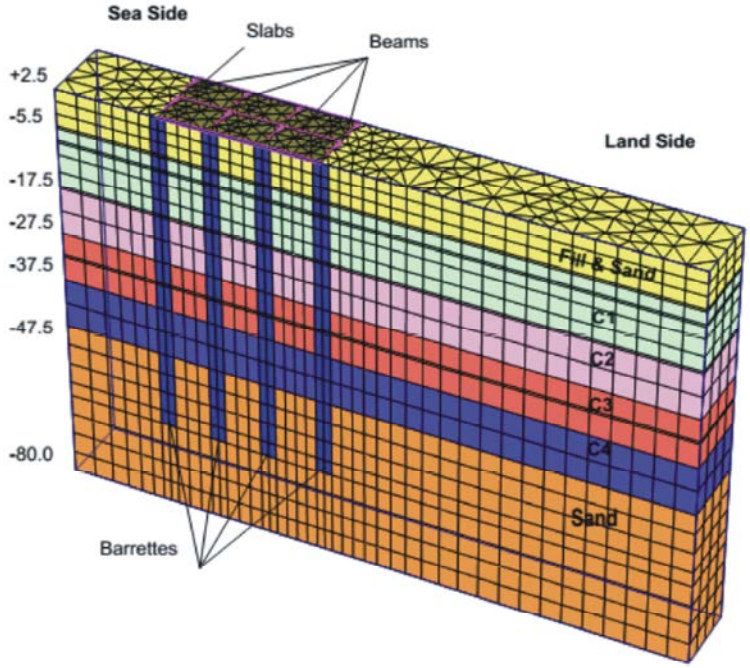

Fig. 8: The generated 3-D mesh of the model (C1 to C4 refer to the four sub-layers of Port-Said Clay)

Structural Elements Properties: The diaphragm walls and slabs had thicknesses of 1.00 and 0.75 m, respectively. Table 1 presents the assigned properties for the different beam systems, which included the main beams connecting the barrettes in each series, the front beam, the back beam and the slab beams.

Construction Phases: The actual construction sequence was described by Hamza *et al*. [16] and followed in this study. Construction involved four main stages as follows:

- Construction of the barrettes, beams and slabs;
- Excavation to the level of -5.0 m LAT;
- Dredging down to the final dredge level of -18.0 m LAT; and
- Application of operational loads.

The operational loads are split in the numerical analysis into two main components as follows:

- Loads acting over the deck and
- Loads acting behind the deck, i.e. behind the back wall.

The loads acting over the deck included a vertical surcharge of 60 kPa. Two vertical line loads of 800 kN/m were also applied from the Gantry Cranes at the lines representing the front and back beams. The two corresponding horizontal line loads were equal to 80 kN/m. The mooring operations on the quay wall were represented by a horizontal force of 2,000 kN every 21 m of the quay wall. Therefore, a line load of 95 kN/m was applied to the 14m-wide numerical model along the line representing the front beam.

The loads acting behind the deck included a vertical surcharge load of 20 kPa for a 30m-wide road directly behind the deck and a vertical surcharge load of 60 kPa until the right boundary. This high surcharge represented the loads from the containers stocks and service operations.

Table 1: Properties of the different beams in the 3D numerical modeling

Property	Main Beam	Front Beam	Back Beam	Slab Beam
Area (A, m^2)	2.4	10.5	9.0	1.0
Unit Weight (kN/m^3)		25		
Young's Modulus (E, kPa)		2×10^7		
Moment of Inertia (I_{22}, m^4)	0.13	10.72	6.75	0.08
Moment of Inertia (I_{33}, m^4)	1.80	7.88	6.75	0.08
Poisson's Ratio (ν, unitless)		0.15		

Table 2: Description of construction phases

Phase number	Description
1	Initial stresses calculated based on the assigned K_0 value for each layer
2	Construction of diaphragm walls
3	Construction of beams
4	Construction of slabs
5	Excavation under deck and in front of it to +0.0 m LAT
6	Excavation under deck and in front of it to -2.5 m LAT
7	Excavation under deck and in front of it to -5.0 m LAT
8	Dredging in front of the deck to -8.0 m LAT
9	Dredging in front of the deck to -11.0 m LAT
10	Dredging in front of the deck to -14.5 m LAT
11	Dredging in front of the deck to -18.0 m LAT
12	Application of operational loads over the deck
13	Application of operational loads behind the deck

Table 3: Summary of the HSM parameters

Layer	Top level (m LAT)	Unit weight (kN/m^3)	K_0	C' (kPa)	ϕ' (deg)	$E_u^{ref}{}_{50}$ (MPa)	m (undrained)	$E^{ref}{}_{50}$ (MPa)	m (drained)	$E^{ref}oed$(Mpa)
Fill & Sand	+2.5	17	0.52	0	29	…	…	20.0	0.5	20.0
C1	-5.5	16	0.59	0	22	4.66	0.81	3.12	0.59	2.1
C2	-17.5		0.64							
C3	-27.5		0.68							
C4	-37.5		0.72							
Sand	-47.5	18	0.43	0	35	…	…	30.0	0.50	30.0

The values of the operational loads were taken according to the Port Operator requirements (Hamza *et al*. [16]).

The numerical simulations proceeded in a total of thirteen phases, as summarized in Table 2. In the initial stresses phase, the initial pore water pressure and the effective vertical and horizontal stresses were calculated. The horizontal effective stresses (σ'_h) were taken equal to the vertical effective stresses (σ'_v) multiplied by the coefficient of at-rest earth pressure (K_o), which was correlated to the plasticity index of Port-Said Clay, as discussed above.

Numerical Analysis Using HSM: The HSM was utilized to simulate the interaction between Port-Said Clay and the quay wall structure in the undrained (short-term) and drained (long-term) conditions. Port-Said Clay was divided into four sub-layers, namely C_1 to C_4, to account for the variation of its plasticity with depth, which in turn affected the value of the at-rest earth pressure coefficient (K_o).

Table 3 summarizes the HSM parameters adopted in this study. Poisson's ratio was assigned values of 0.49 and 0.3 in the undrained and drained conditions, respectively. A default value of 0.2 was adopted for Poisson's ratio during unloading-reloading (ν_{ur}). The interface elements roughness coefficient (R_{inter}) was assigned values of 1.0 for the sub-layers C_1 and C_2, 0.85 for the sub-layers C_3 and C_4 and 0.67 for the fill and sand layers.

Undrained behavior of East Port-Said Port's quay wall using the HSM: The undrained analysis was carried out according to the effective stress approach where the drained shear strength parameters are utilized and the numerical model accounts for the induced pore pressure during different loading conditions. Figure 9 shows the deformed mesh of the structure in the undrained conditions. Figure 10 shows the variations with level of the horizontal movements of the middle, left and right barrettes, which were also equal to the front wall horizontal movement down to the tip level of the wall

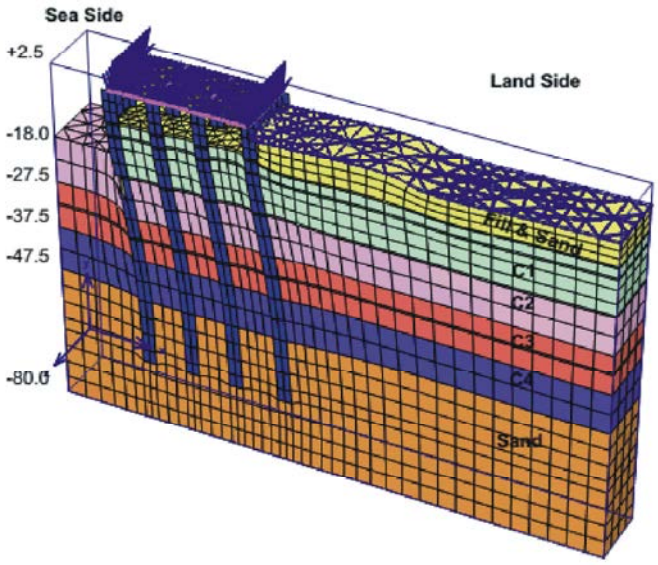

Fig. 9: Deformed mesh of East Port-Said Port's quay wall in the undrained conditions using the HSM (50x)

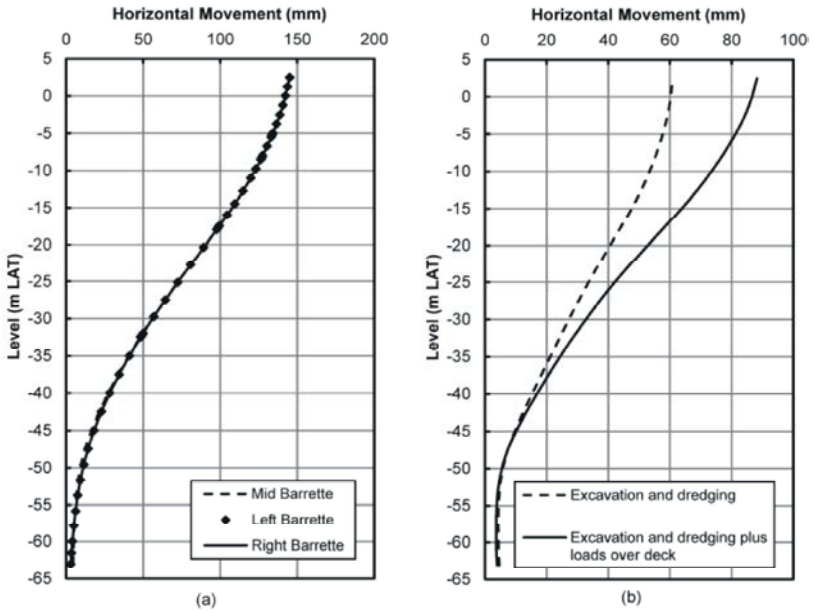

Fig. 10: Variations with level of the horizontal movements in the short-term using the HSM parameters; (a) movement of middle, left and right barrettes under full loads and (b) movement of the middle barrette during construction and due to loads over the deck

at -32 m LAT. The results show that the horizontal movements of the middle, left and right barrettes were equal, which indicates a rigid behavior of the quay wall system.

Figure 10-a presents the horizontal movement due to the accumulated effects of excavation, dredging, the operational loads over the deck and the operational loads behind the deck. Figure 10-b shows the horizontal movement of the middle barrette due to excavation and dredging and due to the accumulated effects of excavation, dredging and the operational loads over the deck. The maximum short-term horizontal movements of the deck structure due to excavation and dredging and due to the accumulated effects of excavation, dredging and the operational loads over the deck equal 61 and 88 mm, respectively. Figure 11 shows the settlement trough behind the back diaphragm wall due to excavation and dredging. The normalized distance and settlement

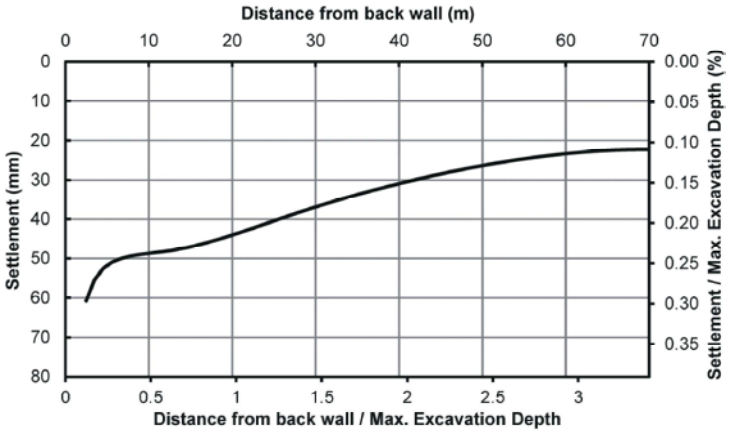

Fig. 11: Settlement trough behind the back wall due to excavation and dredging in the undrained conditions using the HSM parameters

Table 4: Undrained horizontal and vertical movement corresponding to each construction phase using the HSM parameters

Phase Number	Horizontal movement (mm)	Settlement (mm)
1	0	0
2	8	33
3	9	38
4	9	42
5	16	36
6	23	34
7	32	32
8	38	35
9	45	40
10	55	55
11	61	61
12	88	87
13	145	125

Table 5: Drained horizontal and vertical movements corresponding to each construction phase using the HSM parameters

Phase Number	Horizontal movement (mm)	Settlement (mm)
1	0	0
2	12	41
3	13	49
4	14	53
5	14	41
6	17	38
7	25	71
8	35	100
9	51	129
10	77	167
11	107	210
12	151	216
13	198	759

values (relative to the excavation depth of 20.5 m) are also shown in Figure 11. The maximum settlement behind the back wall due to excavation and dredging was 61 mm, which corresponds to a settlement ratio of 0.3%. The relatively high settlement at a distance of 70 m from the back wall is attributed to the inability of the HSM to capture the low strain effects on the soil modulus. Table 4 shows the undrained horizontal wall movement and settlement corresponding to each phase. The results indicate that the maximum settlement due to excavation and dredging equals the maximum horizontal wall movement, which agrees with Gue and Tan [17] for the case of soft to firm clays.

Drained behavior of East Port-Said Port's quay wall using the HSM: The long-term drained behavior of East Port-Said Port's quay wall was investigated by utilizing the drained deformation moduli presented in Table 3. The deformation pattern was similar to the undrained condition but with different magnitudes. The maximum horizontal movement of the front diaphragm wall was 198 mm and the maximum ground settlement behind the deck was 759 mm due to the accumulated effects of excavation, dredging, operational loads over the deck and operational loads behind the deck. The significant increase of the vertical ground movement is clearly attributed to the consolidation of Port-Said Clay, which is considered fully achieved in drained analyses. Table 5 shows the drained horizontal movement and settlement values corresponding to each phase.

Numerical Analysis Using the SSCM: The SSCM was utilized to simulate the long-term behavior of East Port-Said Port's quay wall. The SSCM offers an additional advantage over the HSM by accounting for secondary consolidation effects, which significantly contribute to the overall deformation of soft soils. The deduced SSCM parameters, together with the effective shear strength

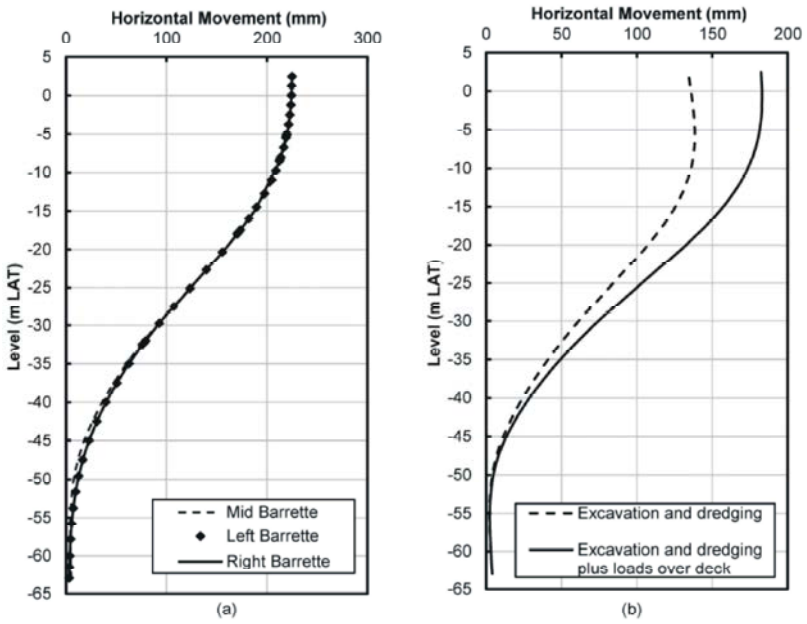

Fig. 12: Variations with level of the horizontal movements in the long-term using the SSCM parameters; (a) movement of middle, left and right barrettes under full loads, (b) movement of the middle barrette during construction and due to loads over the deck

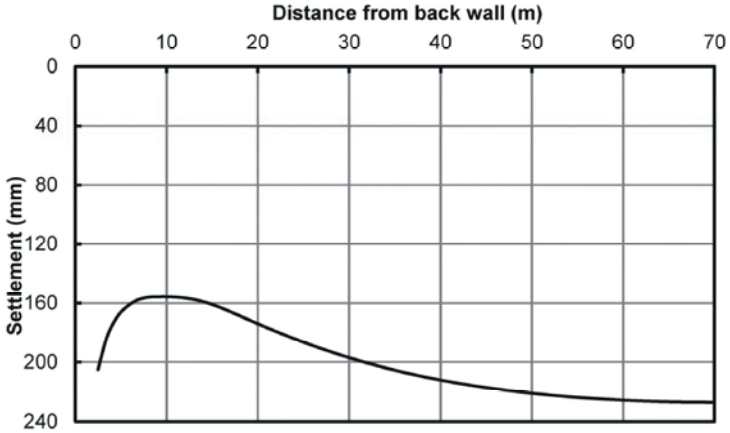

Fig. 13: Vertical movement behind the back diaphragm wall due to excavation and dredging in the drained analysis using the SSCM parameters

parameters, were utilized in the analyses. The cohesionless soils were modeled using the HSM parameters presented in Table 3.

The maximum horizontal movement of the deck structure was 225 mm and the maximum vertical ground movement (settlement) behind the deck was 1.05 m due to the accumulated effects of excavation, dredging, operational loads over the deck and operational loads behind the deck. Figure 12 shows the variation with level of the horizontal movement of the middle, the left and the right barrettes. Figure 12-a presents the movement due to the accumulated effects of excavation, dredging, operational loads over the deck and operational loads behind the deck. Figure 12-b presents the horizontal movement of the middle barrette due to excavation and dredging and due to the accumulated effects of excavation, dredging and the operational loads over the deck. Figure 13 shows the settlement trough behind the back wall due to excavation and dredging only. Table 6 shows the horizontal movement and settlement values corresponding to each phase.

Table 6: Horizontal and vertical movements corresponding to each construction phase using the SSCM parameters

Phase Number	Horizontal movement (mm)	Settlement (mm)
1	0	0
2	9	70
3	11	109
4	12	136
5	15	157
6	20	173
7	28	271
8	40	351
9	60	389
10	94	441
11	134	502
12	182	511
13	225	1050

DISCUSSION

This paper presents a numerical study on the behavior of the existing quay wall of East Port-Said Port considering the short and long-term behaviors of Port-Said Clay utilizing two constitutive models: the Hardening Soil Model (HSM) and the Soft Soil Creep Model (SSCM). The HSM was utilized to model Port-Said Clay behavior in the undrained (short-term) and drained (long-term) conditions. The SSCM was utilized to model the long-term behavior only of Port-Said Clay taking into consideration the secondary consolidation effects.

Figure 14 shows the development of the undrained and drained maximum horizontal wall movement and maximum settlement with the construction phases based on the results of the HSM. The figure shows that the maximum horizontal wall movement due to excavation and dredging increased from 61 mm in the undrained condition to 107 mm in the drained condition; i.e. the percentage of increase equals 75%. The maximum horizontal wall movement due to application of the operational loads (over and behind the deck) has slightly increased from 84 mm in the undrained condition to 91 mm in the drained condition.

The settlement behind the deck due to excavation and dredging increased from 61 mm in the undrained condition to 210 mm in the drained condition, which corresponds to an increase of 244%. The settlement due to application of the operational loads (over and behind the deck) increased from 64 mm in the undrained condition to 549 mm in the drained condition, which corresponds to a percentage of increase of 758%.

The difference between the undrained and drained movements in the HSM represents the effect of primary consolidation of Port-Said Clay, exclusive of any secondary consolidation effects. The primary consolidation effect on vertical movements is more pronounced than on horizontal movements.

The long-term behavior of East Port-Said Port's quay wall was investigated by modeling Port-Said Clay using the HSM and the SSCM, in order to quantify the contribution of secondary consolidation to the long-term deformation behavior of the quay wall. Figure 15 presents the development of the long-term maximum horizontal wall movement and the maximum settlement using the HSM

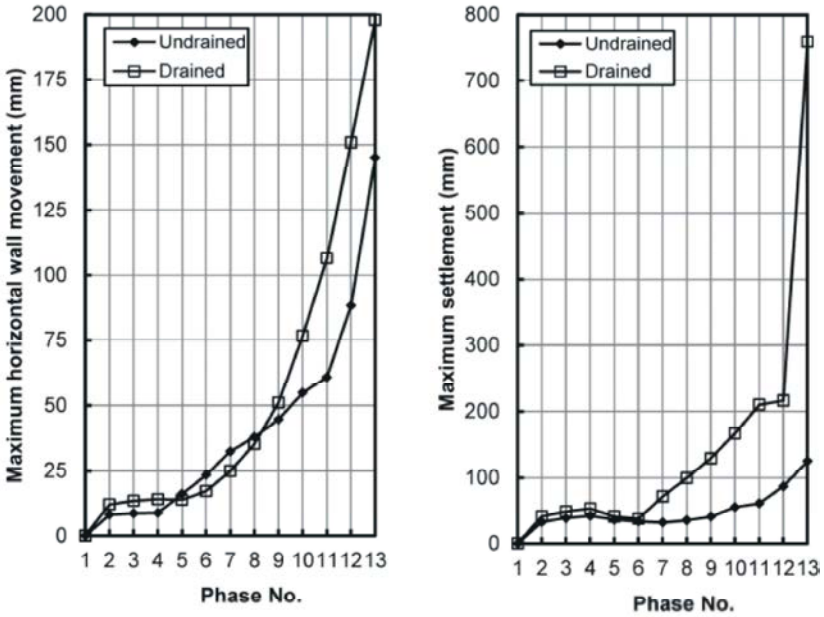

Fig. 14: Comparison between undrained and drained movements using the HSM parameters

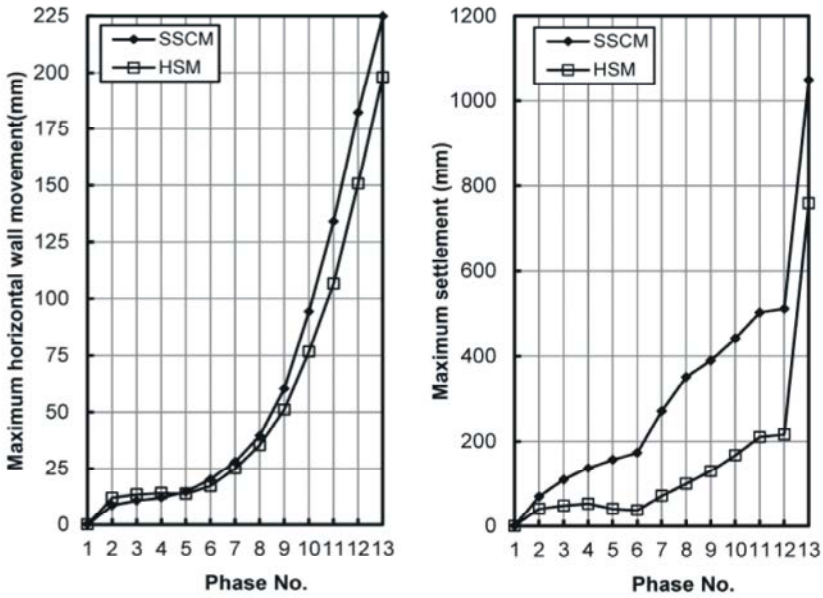

Fig. 15: Comparison between the drained behavior of Port-Said Clay using the HSM and the SSCM parameters

and SSCM parameters. As expected, the predicted movements using the SSCM were higher than those predicted by the HSM. The difference between the two curves represents the secondary consolidation effect on deformation. The results indicate that the maximum horizontal wall movement due to excavation and dredging increased from 107 to 134 mm; i.e. the additional secondary compression represented about 25% of the long-term horizontal wall movement. The maximum horizontal wall movement due to application of the operational loads (over and behind the deck) was equal using the two models.

The settlement behind the deck due to excavation and dredging increased from 210 mm to 502 mm; i.e. the additional secondary compression represented about 139% of the long-term vertical ground movement. The predicted maximum vertical movement by the SSCM due to application of the operational loads (548 mm) was almost equal to that predicted by the HSM.

The insignificant contribution of secondary compression to the operational horizontal and vertical movements is attributed to the fact that the problem is essentially an unloading problem. Hence, the effect of the additional operational loads is primarily governed by the unloading-reloading modulus rather than the primary compression index.

Hamza *et al*. [16] carried out a three-dimensional analysis for East Port-Said Port's quay wall utilizing the finite difference method. A 7-meter-long stretch of the quay wall was simulated under undrained and drained conditions. The soil behavior was modeled using an elastic perfectly plastic model where the yield conditions were defined by Mohr-Coulomb failure criterion. Additional two-dimensional analyses were performed by Hamza *et al*. [16] utilizing the modified Cam Clay model. The calculated maximum horizontal wall movements at the deck level were around 120 and 70 mm under undrained and drained conditions, respectively.

The elastic perfectly plastic constitutive model does not account for the dependency of the soil stiffness on the stress level during primary loading or the effects of unloading and reloading on the soil stiffness, as opposed to the HSM and the SSCM. The results of the present research focus on the importance of modeling soft soils using a more sophisticated constitutive model that accounts for the ongoing secondary consolidation, which is not accounted for by the HSM.

Despite the remarkable advantage of the SSCM in the drained (long-term) conditions, it cannot be utilized to predict the undrained (short-term) behavior. Therefore, the HSM should be used to model the undrained (short-term) behavior and the SSCM should be utilized to model the drained (long-term) behavior of soft soils.

The quay wall under investigation is essentially a three-dimensional structure and the analyses presented in the present research considered the nature of the structure. However, three-dimensional analysis is not always feasible in engineering projects due to cost and time considerations. Design engineers develop two-dimensional idealizations in order to provide a quick and

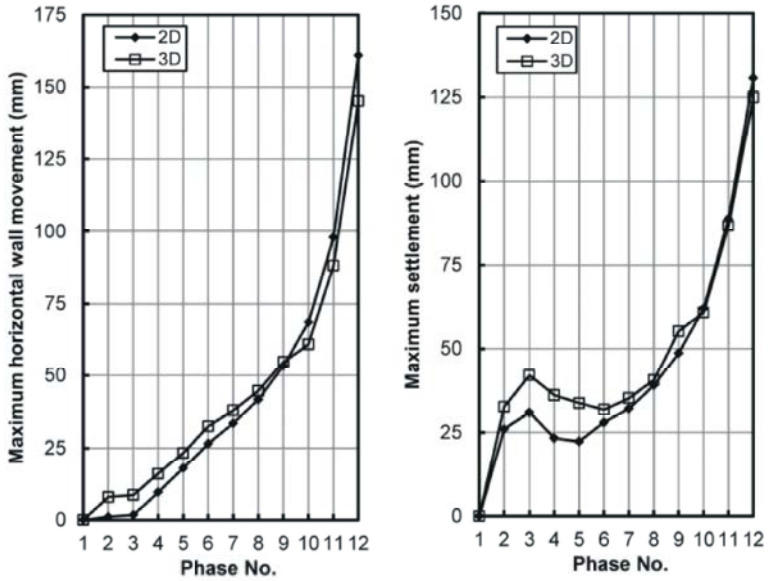

Fig. 16: Comparison between the 2D and 3D analyses of the undrained behavior of Port-Said Clay using the HSM

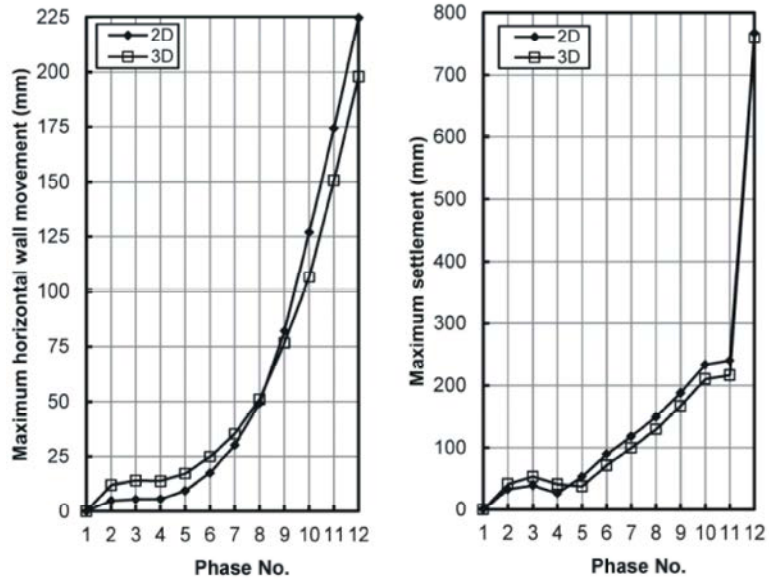

Fig. 17: Comparison between the 2D and 3D analyses of the drained behavior of Port-Said Clay using the HSM

reasonable understanding of the wall behavior. However, the differences between three- and two-dimensional analyses predictions are not known.

It is attempted in this study to idealize the inherently-three-dimensional problem using a two-dimensional (2D) plane strain model. The finite element-based PLAXIS-2D software was utilized to model the same quay wall. One series of barrettes was modeled. The equivalent inertias and areas for the front and back walls, the attached barrettes and the main beam connecting the barrettes and the top slab were calculated. Idealized properties of the front wall and the attached barrettes were used till the tip level of -32.0 m LAT and the properties of the barrettes were utilized from the level of -32 to -60 m LAT. The same was done for the back wall and barrettes but till the tip level of -8.0 m LAT.

The 2D analysis was carried out by utilizing both the HSM and the SSCM and the 2D and 3D analyses results were compared. Figure 16 shows a comparison between the 2D and 3D predictions of the maximum horizontal wall movement and the maximum settlement in different construction phases under undrained conditions using

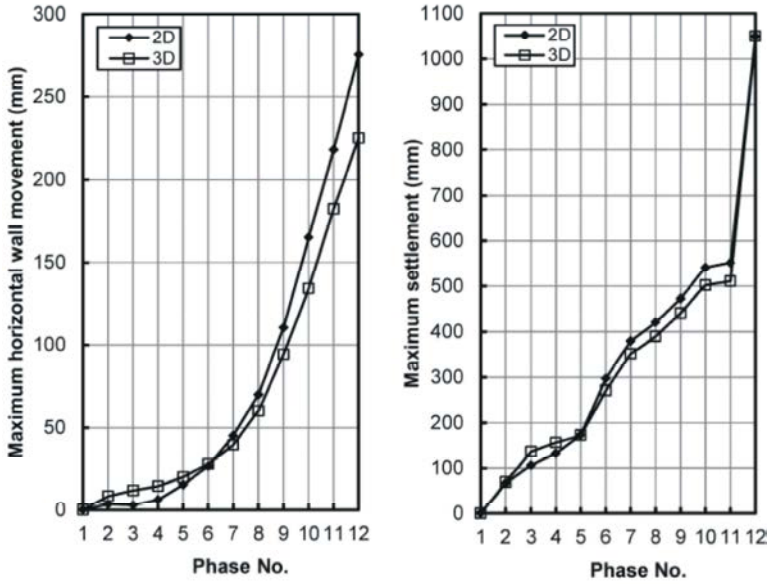

Fig. 18: Comparison between the 2D and 3D analyses of the drained behavior of Port-Said Clay using the SSCM

the HSM parameters. The 3D model consisted of 13 phases with two separate phases for the construction of beams and the construction of slabs. Through the 2D model, the section representing the beams and slabs was idealized. Accordingly, the 2D model consisted of 12 phases with a single phase for the construction of beams and slabs. In order to compare the results of both models, the calculated movements from the phase of construction of beams and the phase of construction of slabs in the 3D model were added together. Hence, the shown number of phases is twelve (12). The predicted maximum horizontal wall movement and maximum settlement from the 2D analysis due to excavation, dredging and operational loads over and behind the deck were 161 and 131 mm, respectively. This represents an increase of 11% and 5% over the corresponding 3D predictions of undrained movement.

Figure 17 shows a comparison between the 2D and 3D predictions of the maximum horizontal wall movement and the maximum settlement in different construction phases under the drained conditions using the HSM parameters. The predicted maximum horizontal wall movement and the maximum settlement from the 2D analysis due to excavation, dredging and operational loads over and behind the deck were 225 mm and 768 mm, respectively. This represents an increase of 14% and 1% over the corresponding 3D predictions of drained movement.

Figure 18 shows a comparison between the 2D and 3D predictions of the maximum horizontal wall movement and the maximum settlement in different construction phases under the drained conditions using the SSCM parameters. The predicted maximum horizontal wall movement and the maximum settlement from the 2D analysis due to excavation, dredging and operational loads over and behind the deck were 275 mm and 1.05 m, respectively. This represents an increase of 22% over the corresponding 3D prediction of the maximum horizontal wall movement. The 2D and 3D predictions of the vertical ground movement in drained conditions were equal.

Two-dimensional analysis overestimates both the horizontal wall movement and the vertical ground movement. The overestimation of the vertical ground movement ranged from zero to 5%, which can be neglected for practical purposes especially under drained conditions. The overestimation of the horizontal wall movement due to excavation, dredging and operational loads (over and behind the deck) was 11% in the undrained condition and was 14 and 22% in the drained condition using the HSM and the SSCM parameters, respectively. The overestimation of the horizontal wall movement occurred despite the observed rigid behavior of the quay wall, as illustrated in Figure 10 and Figure 12.

The assessment of East Port-Said Port's quay wall should be based on the serviceability point of view. The maximum 3D horizontal wall movements due to application of the operational loads over and behind the deck were 84, 91 and 91 mm using the undrained HSM, the drained HSM

and the drained SSCM parameters, respectively. The corresponding 2D values were 93, 98 and 110 mm. This corresponds to a percentage of increase ranging from 8 to 21% over the corresponding 3D prediction of the maximum horizontal wall movement. The allowable horizontal deflection under operation for the maritime structures is 100 mm, according to the BS 6349-2:2010 [18]. Hence, the existing quay wall system in East Port-Said Port satisfied the serviceability requirements.

CONCLUSIONS

The analyses conducted in this study and the interpretation of their results have enabled performing a complete characterization of Port-Said Clay in terms of the numerical simulation of its interaction with a complex structure like the existing quay wall of East Port-Said Port. This study thereby fills a gap in the state of practice in Egypt and represents a significant progress for the development plans in El-Tina Plain region. A full set of design parameters is readily available for use by geotechnical researchers and practitioners. This will enable a reliable prediction of the behavior of other structures and earth embankments resting on Port-Said Clay.

Despite the fact that no field measurements were available to validate the results of numerical modeling, the relative magnitudes of the undrained and drained deformations helped to understand and quantify the effects of primary and secondary consolidation on the deformation behavior. The horizontal wall movement ratio due to excavation and dredging and the horizontal to vertical movement ratio were in line with reported values in the literature for soft to firm clays. Primary consolidation accounts for more than seven times the undrained (short-term) settlement behind the wall under operational loading conditions. Secondary consolidation causes an increase of the long-term horizontal and vertical wall movements due to excavation and dredging by about 25% and 139%, respectively. Primary and secondary consolidation effects are generally more pronounced on vertical ground movements due to excavation and dredging.

Further, the cross-checks carried out considering two-dimensional idealization were useful to predict the three-dimensional behavior from two-dimensional analyses. The results indicated that two-dimensional analyses overestimate the horizontal deflection by up to 22% when adopting a constitutive model that accounts for secondary consolidation effects.

REFERENCES

1. El Gammal, A., 2013. Implication of Holocene Catastrophic Tectonic Activities on Archaeological Sites at Mediterranean Shore North West Sinai Egypt. The Australian Journal of Basic and Applied Sciences,
2. Weir, A.H., E.C. Ormerod and I.M. El Mansey, 1975. Clay mineralogy of sediments of the western Nile Delta. Clay minerals, 10: 369-386.
3. Ibrahem, W.A., 2002. Environmental geology and environmental geophysics of northern Nile Delta in terms of neotectonics and physical processes. A thesis submitted in partial fulfillment for the degree of master of science in geology, Damietta Faculty of Science,
4. Stanley, J., 2003. Nile Delta margin: failed and fluidized deposits concentrated along distributary channels. Geomorphologie: relief, processus, environment, 4: 211-226.
5. Abdeltawab, S. and A. Hussein, 2008. Sahl Al-Tina problematic clay soils and their engineering treatment (northern Sinai Peninsula, Egypt). M.E.R.C. Ain Shams University, Earth Science Series, 22: 202-210.
6. Barakat, M.K., 2010. Modern geophysical techniques for constructing a 3D geological model on the Nile Delta, Egypt. Berlin,
7. Ismail, A. and N. Ryden, 2012. Engineering geological characteristics of soil materials, east Nile Delta, Egypt. International journal of environmental, chemical, ecological, geological and geophysical engineering, 6(5).
8. Hamed, O., M. Mansour, A. Abdel-Rahman and F. El-Nahhas, 2017. Geotechnical Characterization of Port-Said Clay. Accepted for publication in the 19th International Conference on Soil Mechanics and Geotechnical Engineering, Seoul,
9. Abu-Al-Izz, M.S., 1971. Land forms of Egypt. The American university in Cairo press,
10. Abdallah, G., 2006. Management of ground water aquifers along the Mediterranean Sea in Sinai Peninsula. The 2nd international conference on water resources & arid environment,
11. Shanz, T., P. Vermeer and P. Bonnier, 1999. The hardening soil model: formulation and verification. Beyond 2000 in computational geotechnics. Rotterdam,
12. Massarsch, KR., 1979. Lateral earth pressure in normally consolidated clay. Proceedings of the 7th ECSMFE, Brighton, England, 2: 245-250.

13. Duncan, J. and C. Chang, 1970. Nonlinear analysis of stress and strain in soils. Journal of the soil mechanics and foundation division, ASCE, 96(SM5): 1629-1652.
14. Roscoe, K.H., A.N. Schofield and A. Thurairajah, Yielding of clays in state wetter than critical. Geotechnique, 13(3): 211-240.
15. Burland, J.B., 1965. The yielding and dilation of clay. Geotechnique, 15(2): 211-214.
16. Hamza, M., B. Vingiani and F. Leoni, 2002. Port Said east port project- deep diaphragm walls for the quay wall construction. The 9th international conference on piling and deep formations, Nice,
17. Gue, S. and Y. Tan, 1998. Design and construction considerations for deep excavation, SSP Geotechnics Sdn Bhd,
18. British Standard: 2010. Maritime works- part 2: code of practice for the design of quay walls, jetties and dolphins. BS 6349-2.